Influential Factors in Safety Design of Aircraft Pneumatic Duct System

Shi Hong[1*], *Cai Yufei*[2]

1. College of Energy and Power Engineering, Jiangsu University of Science and Technology, Zhenjiang 212003, P. R. China;
2. College of Aerospace Engineering, Nanjing University of Aeronautics and Astronautics, Nanjing 210016, P. R. China

(Received 20 August 2015; revised 13 October 2016; accepted 28 November 2016)

Abstract: The reliability and safety of the pneumatic ducts are essential for flight safety. A beam element model of the duct system is developed and the factors that impact the stress performance of the duct system are investigated, such as stress check standards, flight acceleration, internal temperature and internal pressure. The results show that the stress synthetic method as the stress check standard can obtain the more safety design results. The maximum stress of straight pipe is affected significantly by the acceleration in a plane perpendicular to straight pipe, while the maximum stress of bend pipe is greatly affected by the acceleration in the direction perpendicular to plane of the bend pipe. Meanwhile, internal pressure has little effect on the maximum stress of bend pipe and straight pipe. Temperature has little effect on the maximum stress of bend pipe while has a big impact on the maximum stress of straight pipe.

Key words: high temperature and pneumatic duct; aircrafts; stresses; beam element; safety design

CLC number: V245.4 **Document code**: A **Article ID**: 1005-1120(2017)02-0220-09

0 Introduction

High temperature pneumatic duct system of the aircraft is bled from the engines, auxillary power unit(APU) and ground responsible for the anti-icing system, environment control system, hydraulic system and so on. The duct system is routed throughout the airframe, wings and engine pylon. The accidental rupture can not only make pressure drop dramatically in the ducts, but also lead to the malfunction of the corresponding system and the equipments around it. Therefore, the reliability and safety of the ducts are very important for flight safety[1-3]. In the flight, the duct system suffers many kinds of loads such as temperature, pressure, acceleration and so on. Also, a set of metallic duct system are containing curved and straight sections, joints, welded parts, valves and etc. Furthermore, the structure of the duct system is complex and connected with the frame of the aircraft. As the key issue of design of the bleed air management systems, the safety design of high temperature pneumatic duct system involves heat-liquid-solid coupling process. Therefore, the safety design is in highly complex analysis.

The finite element method was widely used for the strength calculation in civilian industries, so we could expand it into pneumatic duct system. The key is to choose the reasonable finite element model and to convert the loads the ducts suffering to their equivalent nodal loads. Also the element model of the relevant key part such as ball joint and heat exchanger should be established. Unfortunately, so little literatures aiming at strength calculation have been referred for maintaining secrecy. The material behaviors of titanium ducts for use in aircraft pneumatic systems have been studied [4-7]. Nayfeh et al. focused on acoustics of aircraft engine-duct systems[8]. Simulations of bleed-air duct rupture have been conducted by using a CFD tool[9]. All

* Corresponding author, E-mail address: shihong@nuaa.edu.cn.

How to cite this article: Shi Hong, Cai Yufei. Influential factors in safety design of aircraft pneumatic duct system [J]. Trans. Nanjing Univ. Aero. Astro., 2017,34(2):220-228.
http://dx.doi.org/10.16356/j.1005-1120.2017.02.220

these works provide some means of use for reference to this paper but not the key techniques.

In this paper, in order to investigate the safety performance of the duct system, the influences such as stress check standards, temperature, pressure, location of the components on the duct system are analyzed based on the beam element model.

1 Pneumatic Duct System

The schematic of the pneumatic duct system is shown in Fig. 1.

Fig. 1 Schematic of typical bleed-air duct system

During service operation, the pneumatic duct system of a commercial aircraft is subjected to thermodynamic and pressure cycles. In the normal flight process, the bleed air from the engine maintains in high temperature and pressure. Sometimes the requirments of the bleed-air system could be much higher than that of the anti-ice and other air demand system. Therefore, after the engine, there are pressure regulator and shut-off valve(PRSOV) and pre-cooler(PCE), responsible for decreasing the pressure and temperature. In the pipeline, there are also some flow control valves such as wing anti-ice valve (WAIV) and flow control valve(FCV). The bleed-air filter and ozone converter are the air treatment equipment responsible for the air supply quality.

2 Beam Element Method

Since working conditions are complex in flight, all these conditions should be concerned in design in advance. In the initial design, solid element model is not sensible enough to simulate hundreds of conditions. Therefore, the beam element model has been widely used in safety and stability analysis of other piping systems[10-11]. Due to the large length-height ratio of the pneumatic duct system, the beam element model can be adopted in the initial design stage to investigate the safety performance and to compensate stress concentration.

2.1 Straight pipe model

According to the principle of virtual displacement, the beam element as the elastomer has the following form[12-14]

$$\iiint \boldsymbol{\varepsilon}^{\mathrm{T}} \boldsymbol{\sigma} \mathrm{d}V = \int_l \boldsymbol{U}^{\mathrm{T}} \boldsymbol{q} \mathrm{d}x + \boldsymbol{a}^{e\mathrm{T}} \boldsymbol{P}_c^e \tag{1}$$

where $\boldsymbol{\varepsilon}$ the strain of the beam element, $\boldsymbol{\sigma}$ the stress of the beam element, $\boldsymbol{U}$ the displacement of the beam element, $\boldsymbol{q}$ the uniformly distributed load applying to the beam element, $\boldsymbol{a}^e$ the vectors of nodal of element, and $\boldsymbol{P}_c^e$ the concentrated load applying to the nodal of element. $\boldsymbol{\sigma}$ and $\boldsymbol{\varepsilon}$ can be expressed as

$$\boldsymbol{\sigma} = \boldsymbol{D}(\boldsymbol{\varepsilon} - \boldsymbol{\varepsilon}_T - \boldsymbol{\varepsilon}_p) \tag{2}$$

$$\boldsymbol{\varepsilon} = \boldsymbol{B}\boldsymbol{a}^e \tag{3}$$

$$\boldsymbol{U} = \boldsymbol{N}\boldsymbol{a}^e$$

where $\boldsymbol{D}$ is the elastic matrix and $\boldsymbol{B}$ the strain matrix.

$$\boldsymbol{D} = \begin{bmatrix} E & 0 & 0 & 0 \\ 0 & E & 0 & 0 \\ 0 & 0 & E & 0 \\ 0 & 0 & 0 & G \end{bmatrix} \tag{4}$$

$$\boldsymbol{B} = \begin{bmatrix} G_1 & & & & & & G_2 & & & & & \\ & G_3 & & & & G_4 & & G_5 & & & & G_6 \\ & & G_7 & & G_8 & & & & G_9 & & G_{10} & \\ & & & G_{11} & & & & & & G_{12} & & \end{bmatrix} \tag{5}$$

And

$G_1 = 1/l, G_2 = 1/l, G_3 = -y(-6/l^2 + 12x/l^3), G_4 = -y(-4/l + 18x/l^2), G_5 = -y(6/l^2 - 12x/l^3), G_6 = -y(-2/l + 6x/l^2), G_7 = -z(-6/l^2 + 12x/l^3), G_8 = -z(-4/l + 18x/l^2), G_9 = -z(6/l^2 - 12x/l^3), G_{10} = -z(-2/l + 6x/l^2), G_{11} = -r/l, G_{12} = r/l$.

$$\boldsymbol{N} = \begin{bmatrix} A_1 & & & & & & A_2 & & & & & \\ & A_3 & & & & A_4 & & A_5 & & & & A_6 \\ & & A_7 & & A_8 & & & & A_9 & & A_{10} & \\ & & & A_{11} & & & & & & A_{12} & & \end{bmatrix} \tag{6}$$

$A_1=1-x/l, A_2=x/l, A_3=1-3x^2/l^2+2x^3/l^3$, $A_3=1-3x^2/l^2+2x^3/l^3, A_4=x-2x^2/l+3x^3/l^2$, $A_5=3x^2/l^2-2x^3/l^3, A_6=-x^2/l+x^3/l^2, A_7=1-3x^2/l+2x^3/l^3, A_8=x-2x^2/l+3x^3/l^2$, $A_9=3x^2/l^2-2x^3/l^3, A_{10}=-x^2/l+x^3/l^2, A_{11}=1-x/l, A_{12}=x/l$.

$$\boldsymbol{\varepsilon}_T=[\alpha\Delta T\ \ 0\ \ 0\ \ 0\ \ 0\ \ 0\ \ \alpha\Delta T\ \ 0\ \ 0\ \ 0\ \ 0\ \ 0]^{\mathrm{T}} \tag{7}$$

$$\boldsymbol{\varepsilon}_p=\left[\frac{1}{E}\left(\frac{PD}{4\delta}-\nu\frac{PD}{2\delta}\right)\ \ 0\ \ 0\ \ 0\ \ 0\ \ 0\ \ \frac{1}{E}\left(\frac{PD}{4\delta}-\nu\frac{PD}{2\delta}\right)\ \ 0\ \ 0\ \ 0\ \ 0\ \ 0\right]^{\mathrm{T}} \tag{8}$$

where E is the elasticity modulus, G the shear elasticity, α the coefficient of linear expansion, ΔT the temperature variation, P the internal pressure, D the radius of the duct, and δ the thickness of the duct.

Substituting Eqs. (2)—(8) into Eq. (1), we can obtain the following expression

$$\iiint \boldsymbol{B}^{\mathrm{T}}\boldsymbol{D}\boldsymbol{B}\boldsymbol{a}^e\mathrm{d}V=\int \boldsymbol{N}^{\mathrm{T}}q\mathrm{d}x+\boldsymbol{P}_c^e+\iiint \boldsymbol{B}^{\mathrm{T}}\boldsymbol{D}\boldsymbol{\varepsilon}_T\mathrm{d}V+\iiint \boldsymbol{B}^{\mathrm{T}}\boldsymbol{D}\boldsymbol{\varepsilon}_p\mathrm{d}V \tag{9}$$

$$\boldsymbol{K}^e=\iiint \boldsymbol{B}^{\mathrm{T}}\boldsymbol{D}\boldsymbol{B}\mathrm{d}V \tag{10}$$

$$\boldsymbol{K}^e=\begin{bmatrix}
\frac{EA}{l} & & & & & & & & & & & \\
0 & \frac{12EI_z}{l^3} & & & & & & & & & & \\
0 & 0 & \frac{12EI_y}{l^3} & & & & & \text{symmetry} & & & & \\
0 & 0 & 0 & \frac{GJ_k}{l} & & & & & & & & \\
0 & 0 & \frac{6EI_y}{l^2} & 0 & \frac{4EI_y}{l} & & & & & & & \\
0 & \frac{6EI_z}{l^2} & 0 & 0 & 0 & \frac{4EI_z}{l} & & & & & & \\
-\frac{EA}{l} & 0 & 0 & 0 & 0 & 0 & \frac{EA}{l} & & & & & \\
0 & -\frac{12EI_z}{l^3} & 0 & 0 & 0 & -\frac{6EI_z}{l} & 0 & \frac{12EI_z}{l^3} & & & & \\
0 & 0 & -\frac{12EI_y}{l^3} & 0 & -\frac{6EI_y}{l} & 0 & 0 & 0 & \frac{12EI_y}{l^3} & & & \\
0 & 0 & 0 & -\frac{GJ_k}{l} & 0 & 0 & 0 & 0 & 0 & \frac{GJ_k}{l} & & \\
0 & 0 & \frac{6EI_y}{l^2} & 0 & \frac{2EI_y}{l} & 0 & 0 & 0 & 0 & 0 & \frac{4EI_y}{l} & \\
0 & \frac{6EI_z}{l^2} & 0 & 0 & 0 & \frac{2EI_z}{l} & 0 & 0 & 0 & 0 & 0 & \frac{4EI_z}{l}
\end{bmatrix} \tag{11}$$

In Eq. (11), $I_y=\iint z^2\mathrm{d}A$ and $I_z=\iint y^2\mathrm{d}A$ are the principal moments of inertia about y-axis and z-axis, respectively. $J_k=\iint r^2\mathrm{d}A$ is the principal moment of inertia about x-axis[15-16].

2.2 Bend pipe model

Due to the compact space layout in the cabin, there are some bends in the pipeline. For the bend, there are three methods in modeling which are bend unit technology, straight pipe replacement technology and elastic hinged model[17-18]. For the small radius of curvature (The radius of curvature and diameter is less than 3), we can choose the last model for high efficiency. Fortunately, in the high temperature pneumatic duct system, the bends almost belong to the small radius of curvature category. The schematic of the bend with small radius of curvature is shown in Fig. 2.

The elbow of the elastic hinged can be seen as flexible structure, the flexural rigidity of the elastic hinged can be expressed as

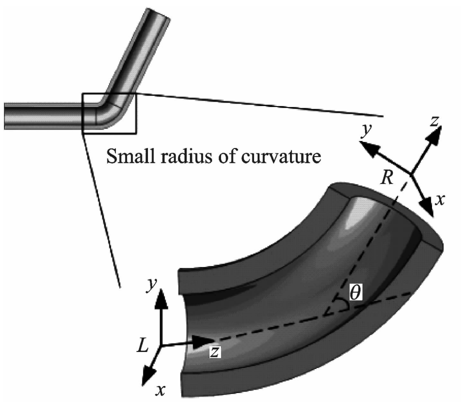

Fig. 2 Schematic of bend with small radius of curvature

$$K=\frac{EJ}{kR\theta} \tag{12}$$

where k is the flexibility factor of the bend, $k=\frac{1.65r^2}{R\theta}$. R is the radius of curvature and θ the intersection angle. J is the rotational inertia, $J=\pi r^2\delta$.

Considering the influences of the internal pressure, the flexural rigidity of the elastic hinged become

$$K=\frac{E\pi r\delta^2}{1.65\theta}\left[1+\frac{6P\cdot r}{E\delta}\left(\frac{r}{\delta}\right)^{4/3}\left(\frac{R}{r}\right)^{1/3}\right] \tag{13}$$

where r is the radius of the pipe.

Element stiffness matrix of the bend is given by

$$\boldsymbol{K}^e=\begin{bmatrix} 10^n &&&&&&&&&&& \\ 0 & 10^n &&&&&& \text{symmetry} &&&& \\ 0 & 0 & 10^n &&&&&&&&& \\ 0 & 0 & 0 & 10^n &&&&&&&& \\ 0 & 0 & 0 & 0 & K &&&&&&& \\ 0 & 0 & 0 & 0 & 0 & K &&&&&& \\ -10^n & 0 & 0 & 0 & 0 & 0 & 10^n &&&&& \\ 0 & -10^n & 0 & 0 & 0 & 0 & 0 & 10^n &&&& \\ 0 & 0 & -10^n & 0 & 0 & 0 & 0 & 0 & 10^n &&& \\ 0 & 0 & 0 & -10^n & 0 & 0 & 0 & 0 & 0 & 10^n && \\ 0 & 0 & 0 & 0 & -K & 0 & 0 & 0 & 0 & 0 & K & \\ 0 & 0 & 0 & 0 & 0 & -K & 0 & 0 & 0 & 0 & 0 & K \end{bmatrix} \tag{14}$$

where n is the particularly large number.

It is worthy of note that the stress of the bend is much larger than that of the straight pipe when they suffer the same load. The ratio of those two kinds of stress is the stress concentration factor which only has the effect on the longitudinal bending stress. According to ASME B31, the stress concentration factor is given by

$$\beta=\frac{0.9}{\lambda^{2/3}} \tag{15}$$

where λ is the flexibility characteristic parameter, $\lambda=R\delta/r^2$.

2.3 Equivalent nodal load

Gravity and acceleration as the uniformly distributed load can be converted to the equivalent nodal load. The schematic of conversion of gravity and acceleration is presented as shown in Fig. 3.

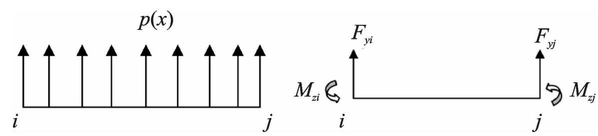

Fig. 3 Schematic of conversion of distributed loads

Then equivalent nodal load of gravity $\boldsymbol{f}_g^e$ is

$$\boldsymbol{f}_g^e=\int[\boldsymbol{N}]^{\mathrm{T}}q_g\,\mathrm{d}x \tag{16}$$

$$q_g=\rho Ag\cos(x,X) \tag{17}$$

$$\boldsymbol{f}_g^e=\begin{Bmatrix}F_{yi}\\M_{zi}\\F_{yj}\\M_{zj}\end{Bmatrix}=\begin{bmatrix}1 & 0 & -\frac{3}{l^2} & \frac{2}{l^3}\\ 0 & 1 & -\frac{2}{l} & \frac{1}{l^2}\\ 0 & 0 & \frac{3}{l^2} & -\frac{2}{l^3}\\ 0 & 0 & -\frac{1}{l} & \frac{1}{l^2}\end{bmatrix}\begin{Bmatrix}\int_0^l q_g\,\mathrm{d}x\\ \int_0^l q_g x\,\mathrm{d}x\\ \int_0^l q_g x^2\,\mathrm{d}x\\ \int_0^l q_g x^3\,\mathrm{d}x\end{Bmatrix}=\begin{bmatrix}-\frac{q_g l}{2}\\ -\frac{q_g l^2}{12}\\ -\frac{q_g l}{2}\\ \frac{q_g l^2}{12}\end{bmatrix} \tag{18}$$

where q_g is the uniformly distributed load of gravity, $\cos(x,X)$ the cosine of the local coordinate system and the global coordinate system, and l the length of the element. F_{yi} and M_{zi} are the force in y-axis and moment in z-axis of node i, F_{yj} and M_{zj} the force in y-axis and moment in z-axis of node j.

And equivalent nodal load of acceleration $\boldsymbol{f}_a^e$ is

$$\boldsymbol{f}_a^e=\int[\boldsymbol{N}]^{\mathrm{T}}q_a\,\mathrm{d}x \tag{19}$$

$$q_a=\rho Aa\cos(x,X) \tag{20}$$

$$\boldsymbol{f}_a^e=\begin{Bmatrix}F_{yi}\\M_{zi}\\F_{yj}\\M_{zj}\end{Bmatrix}=\begin{bmatrix}-\frac{q_a l}{2}\\ -\frac{q_a l^2}{12}\\ -\frac{q_a l}{2}\\ \frac{q_a l^2}{12}\end{bmatrix} \tag{21}$$

where q_a is the flight acceleration.

2.4 Global stiffness matrix and nodal load matrix of duct system

After all the element stiffness matrix is developed, we can obtain the global stiffness matrix by superposition method and expanding matrix method. Assuming that the number of the nodes is n, the global stiffness matrix $\boldsymbol{K}^e_{6n\times 6n}$ can be expressed as

$$\boldsymbol{K}^e_{6n\times 6n}=\begin{bmatrix} & \vdots & & \vdots & \\ \cdots & K_{ii} & \cdots & K_{ij} & \cdots \\ & \vdots & & \vdots & \\ \cdots & K_{ji} & \cdots & K_{jj} & \cdots \\ & \vdots & & \vdots & \end{bmatrix} \tag{22}$$

In Eq. (22), the dot and blank in the matrix represent the six-by-six zero matrix. The node numbers i and j are listed in an ascending order. Sub-matrixes of the element matrix are added into the global matrix by superposition method. For the nodal force, the superposition method is also used

$$\boldsymbol{f}=\sum_{e=1}^{n_e} f^e \tag{23}$$

Then we obtain the global equilibrium equations

$$\boldsymbol{K\delta}=\boldsymbol{f} \tag{24}$$

where $\boldsymbol{f}$ is the global nodal force matrix, $\boldsymbol{\delta}$ the global nodal displacement matrix, $\boldsymbol{K}$ the global stiffness matrix. It can be known that $\boldsymbol{K}^e_{6n\times 6n}$ is a singular matrix, So Eq. (24) can be solved by method of multiplication by a large number.

2.5 Computational flow diagram

Computational flow diagram is shown in Fig. 4.

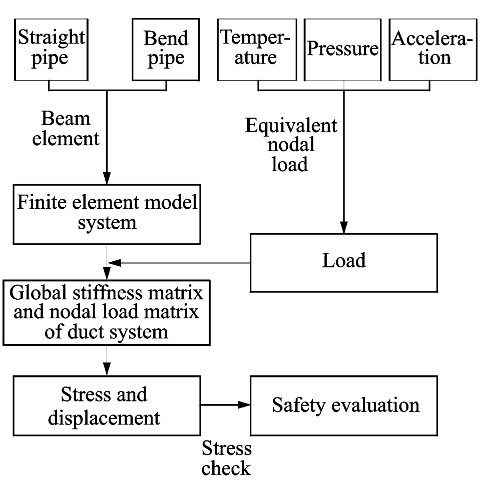

Fig. 4 Computational flow diagram

3 Analysis of Influence Factors

Prior to the analysis, material properties of the duct are given. The duct is made of CRES 321 (A312 TP321). The density ρ of CRES 321 is 7 900 kg/m^3 and Poisson's ratio ν is 0.3. The other properties of CRES 321 are shown in Table 1, where F_{TU} is the plastic limit and F_{TY} the yield limit.

Table 1 Properties of CRES 321

Temperature/ ℃	E/ MPa	α/ (mm · ℃)$^{-1}$	F_{TU}/ MPa	F_{TY}/ MPa
20	195 000	16.00E-6	665	200
200	186 000	16.50E-6	515	157
300	179 000	17.00E-6	490	147
500	165 000	18.00E-6	413	119

3.1 Stress check standard

There are two kinds of stress check standards evaluating the stress of the high temperature pneumatic duct system, which are stress classification method and stress synthetic method.

(1) Stress classification method

Stress classification method divides the stress into two kinds, namely the primary stress and secondary stress. The checking formulas of the primary stress are given by

$$\sigma_L=\frac{PD}{4\delta}+\frac{0.75 i_s M_A}{W}\leqslant[\sigma]^h \tag{25}$$

$$\sigma_{LO}=\frac{PD}{4\delta}+\frac{0.75 iM_A}{W}+\frac{0.75 iM_B}{W}\leqslant 1.2[\sigma]^h \tag{26}$$

where σ_L is the sum of the longitudinal stress resulting from the sustained load such as pressure, gravity and acceleration, $[\sigma]^h$ the allowable stress of longitudinal stress, i_s the stress intensity factor, M_A the sum of the bending moment resulting from the pressure and gravity, W the modulus of section, σ_{LO} the one kind of the primary stress resulting from accidental load such as wind, earthquake and vibration, and M_B the bending moment resulting from accidental load.

The checking formula of the secondary stress is given by

$$\sigma_E=\frac{0.75 iM_C}{W}=[\sigma_E]\leqslant f(1.25([\sigma]^c+[\sigma]^h)-\sigma_L) \tag{27}$$

where σ_E is the displacement stress resulting from thermal expansion and contraction and the joint displacement, M_C the bending moment resulting from thermal expansion, $[\sigma_E]$ the allowable stress of secondary stress, and $[\sigma]^c$ the allowable stress in room temperature.

(2) Stress synthetic method

According to distortion energy theory, the checking formula of stress synthetic method can be expressed as

$$\sqrt{\frac{1}{2}(\sigma_1-\sigma_2)^2+(\sigma_2-\sigma_3)^2+(\sigma_3-\sigma_1)^2}\leqslant[\sigma] \tag{28}$$

where σ_1, σ_2, σ_3 are the three principal stresses in three directions, respectively. $[\sigma]$ is the allowable stress of stress synthetic method.

(3) Comparison of two methods

To compare the two methods in safety design, we take a set of the duct in trim system as an example, which is shown in Figs. 5, 6. The internal temperature is 220 ℃, the internal pressure is 0.8 bar. In that situation, $[\sigma]^h$ is 155.0 MPa, $[\sigma_E]$ is 282.8 MPa, $[\sigma]$ is 155.0 MPa. From Fig. 7, we can see that the primary stress and secondary stress are less than those of the allowable stress value. Von Mises stress of Node 5 and Node 6 in the same situation is greater than the allowable stress value 155.0 MPa corresponding to allowable stress of secondary stress. Therefore, different stress check standards can obtain different results. Considering the high requirements for the safety and reliability, we suggest the stress synthetic method for safety checking work to obtain the more safety design results.

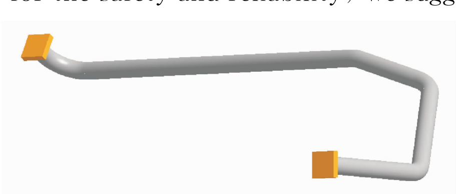

Fig. 5 A set of the duct in trim system

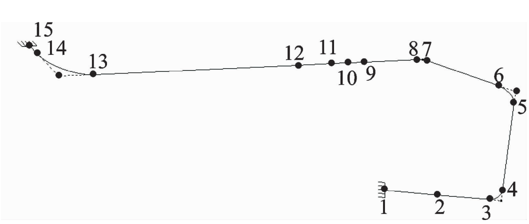

Fig. 6 Node number of the duct

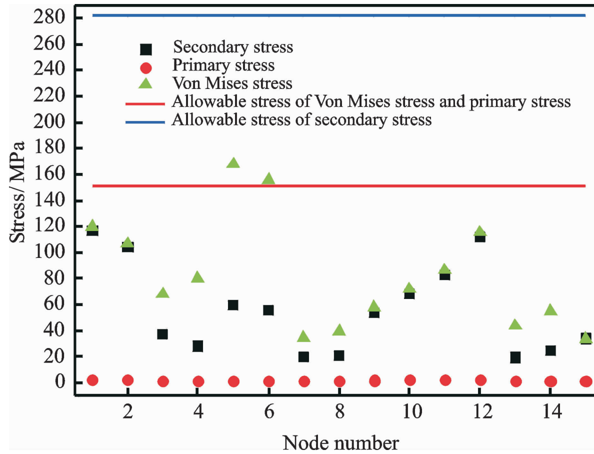

Fig. 7 Comparison of the stress results using two stress check standards

3.2 Flight acceleration

The high temperature pneumatic duct system can be divided into two kinds of structure, which are straight pipe and bend pipe. Therefore, we choose straight pipe and bend pipe as the study objects to investigate the influences of the following influencing factors on safety design. The diameter of the pipe is 38.1 mm, the internal pressure is 0.8 bar, and the internal temperature is 60 ℃. The direction of gravity is vertically downward, that is z-axis in Figs. 8, 9.

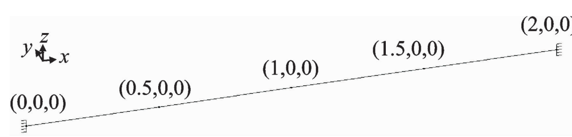

Fig. 8 straight pipe

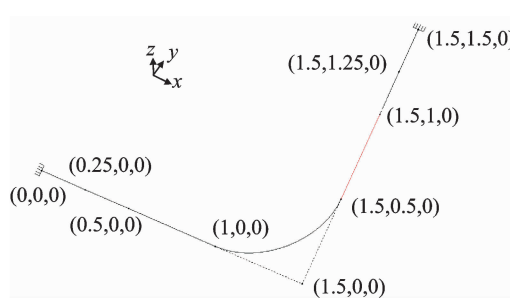

Fig. 9 Bend pipe

In flight, the aircraft are not only subject to the pressure, temperature and nodal displacement load, but also suffering the acceleration load. In order to investigate the influence of acceleration load on the stress performance, we study the stress performances of straight pipe and bend pipe in the x, y and z direction under acceleration load. The influences of acceleration load on the maximum stress of straight pipe and bend pipe are shown in Figs. 10, 11.

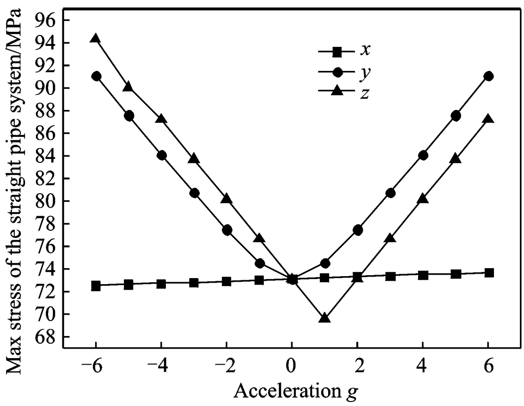

Fig. 10 Influence of acceleration on the max stress of straight pipe

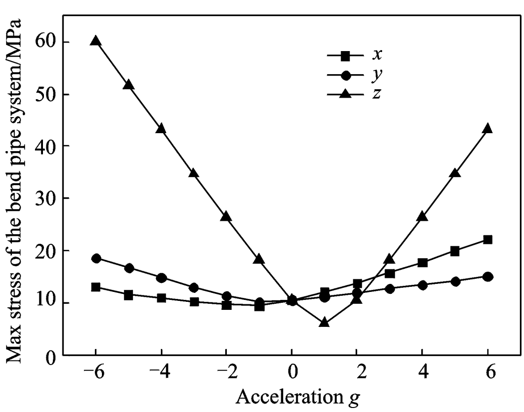

Fig. 11 Influence of acceleration on max stress of the bend pipe

In Fig. 10, the acceleration in x direction has little effect on the maximum stress of straight pipe while acceleration in y and z direction makes a big impact on the maximum stress of straight pipe. Meanwhile, the maximum stress of straight pipe decreases first and then increases with acceleration from $-6g$ to $6g$. Therefore, the maximum stress of straight pipe is greatly affected by the acceleration in a plane perpendicular to straight pipe.

From Fig. 11, we can see that acceleration in x and y direction has little effect on the maximum stress of bend pipe while acceleration in z direction makes a big impact on the maximum stress of bend pipe. Meanwhile, the maximum stress of bend pipe decreases first and then increases with acceleration from $-6g$ to $6g$, and such effect of acceleration on the bend pipe is more serious than that in straight pipe. Therefore, for the bend pipe, the maximum stress of bend pipe is greatly affected by the acceleration in the direction perpendicular to plane of the bend pipe.

3.3 Internal pressure

To transport the air to the downstream system, the bleed air has a certain pressure of up to 10 bar. Therefore, we take pressure as a variable and keep the temperature and acceleration constant. The temperature is 60 ℃ and the acceleration is 0.

As is shown in Fig. 12, when the internal pressure increases from 0.8 bar to 8.8 bar, it can be seen that internal pressure has little effect on the maximum stress of bend pipe and straight pipe although the maximum stress increases with the internal pressure. Therefore, it tells us that we should not focus on the internal pressure when conducting the safety design.

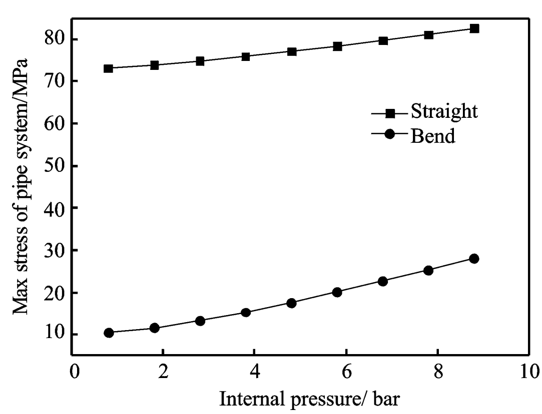

Fig. 12 variation of the max stress of the duct system with the internal pressure

3.4 Gas temperature

The air in the duct system is at high temperature of up to 260 ℃. Therefore, we take temperature as variable and keep the pressure and acceleration constant. The pressure is 0.8 bar and the acceleration is 0.

As is shown in Fig. 13, temperature has little effect on the maximum stress of bend pipe while it makes a big impact on the maximum stress of straight pipe. Meanwhile, the maximum stress of bend pipe and straight pipe increases with temperature from 50 ℃ to 90 ℃. Combined Eqs. (1), (2) and (7), we have the beam element stress depending on the temperature, pressure and distribution load. From the Fig. 12, we obtain that internal pressure load has little effect on the maximum stress of bend pipe and straight pipe. And from the Figs. 10, 11, we know the acceleration with 1g in x, y and z directions has little effect on the maximum stress of straight pipe. Therefore, the maximum stress of straight pipe mainly depends on the temperature. Eq. (7) tells us the strain of the beam element shows significant linear correlations with temperature. That is the reason why the maximum stress of straight pipe almost linear increases with temperature. Therefore, it tells us that it is essential to pay more attention to the straight pipe in the high temperature compared with the pressure.

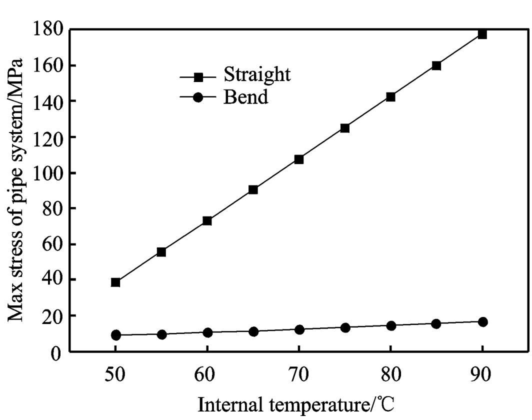

Fig. 13 Variation of the max stress of duct system with internal temperature

4 Conclusions

The main aim of this paper is to investigate the influences such as stress check standards, flight acceleration, internal temperature and internal pressure on the stress performance of the duct system from the numerical point of view. Key findings and conclusions from the simulation studies performed are as follows:

(1) Different stress check standards can obtain different results. Considering the high requirements for the safety and reliability, we suggest the stress synthetic method for safety checking work to obtain the more safety design results.

(2) The maximum stress of straight pipe is greatly affected by the acceleration in a plane perpendicular to straight pipe while the maximum stress of bend pipe is greatly affected by the acceleration in the direction perpendicular to plane of the bend pipe.

(3) It can be seen that internal pressure has little effect on the maximum stress of bend pipe and straight pipe although the maximum stress increases with the internal pressure. Therefore, it tells us that we should not focus on the internal pressure when conducting the safety design.

(4) Temperature has little effect on the maximum stress of bend pipe while impacting significantly on the maximum stress of straight pipe. Therefore, it tells us that it is essential to pay more attention to the straight pipe at high temperature in the safety design.

Acknowledgements

My deepest gratitude goes to the engineers of Shanghai Aircraft Design & Research Institute for their cooperation in releasing the data for publication and technical support.

References:

[1] SHI Hong, JIANG Yanlong, ZHONG Wei, et al. Effect of bleed air ducts on flow and heat transfer in aircraft enclosed space [J]. Journal of Nanjing University of Aeronautics & Astronautics. 2012, 44(3): 313-319. (in Chinese)

[2] SHI Hong, JIANG Yanlong, LIU Zhili, et al. Simulation of bleed air behavior during aircraft in flight based on flowmaster[J]. Transactions of Nanjing University of Aeronautics and Astronautics, 2013, 30(2):132-138. (in Chinese)

[3] LIU Juan, JIANG Yanlong, SHI Hong, et al. Modal analysis of the high temperature and pneumatic duct system of the aircraft [J]. Advanced Materials Research, 2013, 663: 552-559. (in Chinese)

[4] ADIB A M L, BAPTISTA C A R P, BARBOZA M J

R, et al. Aircraft engine bleed system tubes: Material and failure mode analysis[J]. Engineering Failure Analysis, 2007,14(8):1605-1617.

[5] BAPTISTA C A R P, BARBOZA M J R, ADIB A M L, et al. High temperature cyclic pressurization of titanium ducts for use in aircraft pneumatic systems [J]. Materials & Design, 2009,30(5):1503-1510.

[6] CARVALHO S M, Baptista C A R P, LIMA M S F. Fatigue in laser welded titanium tubes intended for use in aircraft pneumatic systems [J]. International Journal of Fatigue, 2016, 90:47-56.

[7] CARVALHO S M, BAPTISTA C A R P, LIMA M S F. Simulating the damage accumulation in aircraft bleed system ducts joined by laser and arc welding processes[J]. Procedia Engineering, 2011, 10(7): 1321-1326.

[8] NAYFEH A H, KAISER J E, TELIONIS D P. Acoustics of aircraft engine-duct systems[J]. AIAA Journal, 1973, 13(2):130-153.

[9] PAPA R, MATTOS B D, SANTOS L C. Simulations of bleed-air duct rupture[C]//21st Applied Aerodynamics Conference. Florida: AIAA, 2003:214-220.

[10] CHEN Guo, LUO Yun, ZHENG Qihui, et al. Fluid-structure coupling dynamic model of complex spatial fluid-conveying pipe system and its verification[J]. Acta Aeronautica et Astronautica Sinica, 2013, 34 (3):597-609. (in Chinese)

[11] LI Lin, YU Lifan. The research trends of fluid-solid coupling vibration problems of piping system[J]. Chinese Journal of Applied Mechanics, 1997, 14(3): 40-48. (in Chinese)

[12] DONG Jun, LIU Xuhong, YAO Shunzhong, et al. Analysis of element stiffness matrix about space beam element based on principle of virtual work[J]. Journal of Southwest Forestry College, 2002, 22(4): 59-62. (in Chinese)

[13] HU Yujin, WANG Zhangqi. Finite element analysis and applications[M]. Beijing: Tsinghua University Press, 2009. (in Chinese)

[14] FAN Qinshan, YIN Yjun. Mechanics of materials [M]. Beijing: Tsinghua University Press, 2008. (in Chinese)

[15] WANG Xucheng. Finite element method [M]. Beijing: Tsinghua University Press, 2007. (in Chinese)

[16] FU Yonghua. Finite element analysis [M]. Wuhan: Wuhan University Press, 2003. (in Chinese)

[17] CUI Xiaobing, TONG Xinghua, CAI Qiangkang. Piping stress analysis and application of spherical compensator [J]. Petrochemical Equipment, 1990, 19 (3):1-4. (in Chinese)

[18] TONG Xinghua, CUI Xiaobing, CAI Qiangkang. Application of elastic flexure hinge model in piping structure analysis [J]. Journal of Petroleum University, 1989, 13(5):51-61. (in Chinese)

Dr. **Shi Hong** received her Ph. D. degree in Man-Machine & Environment Engineering from Nanjing University of Aeronautics and Astronautics, Nanjing, China, in 2013. From 2013 to present, she has been with College of Energy and Power Engineering, Jiangsu University of Science and Technology in Zhenjiang. Her research has focused on efficient heat-exchanging technology and aircraft environmental control technology.

Dr. **Cai Yufei** received his Ph. D. degree in Man-Machine & Environment Engineering from Nanjing University of Aeronautics and Astronautics, Nanjing, China, in 2016. From 2016 to present, he begins postdoctoral research with Nanjing University of Aeronautics and Astronautics. His research has focused on efficient heat-exchanging technology and aircraft environmental control technology.

(Executive Editor: Xu Chengting)